CAUCHY – Jurnal Matematika Murni dan Aplikasi
Volume 11 (1) (2026), Pages 667-682
p-ISSN: 2086-0382; e-ISSN: 2477-3344

Dynamics of a Stage-Structured Predator–Prey Model with Holling Type II Functional Response and Cannibalism

Sela Tri Indah Sari and Dian Savitri*

Department of Mathematics, Faculty of Mathematics and Natural Sciences, Universitas Negeri Surabaya, Indonesia

Abstract

Predator–prey models with nonlinear functional responses provide a robust framework for population regulation. This study analyzes a three-dimensional model incorporating a Holling type II functional response, predator stage structure, and cannibalism. While many models simplify predator development, this work examines the interplay between maturation and stage-specific interactions. Analytical conditions for the existence of a positive coexistence equilibrium are derived from the positivity of the steady-state solutions, while its local stability is established using the Routh–Hurwitz criteria. To validate these, numerical simulations were performed via Python's SciPy solver, demonstrating convergence to a stable coexistence equilibrium $(59.9078, 23.9092, 56.0552)$ for the baseline parameter set, which is consistent with the derived analytical conditions. Stability transitions were investigated through numerical continuation in MatCont (MATLAB). For the adult predation rate m_1, two Hopf points were identified at 0.4211 and 8.7725, representing supercritical and subcritical bifurcations, respectively. Conversely, the maturation rate m induces supercritical Hopf bifurcations at 0.2661 and 0.5271, while cannibalism triggers a supercritical Hopf point at 0.1835. These findings show maturation and cannibalism define distinct instability thresholds, while varying predation intensity induces stable and unstable periodic regimes in stage-structured populations.

Keywords: Cannibalism; Holling Type II Functional Response; Hopf Bifurcation; Numerical Continuation; Stage-Structured Predator–Prey Model

1. Introduction

Predator–prey interactions constitute a fundamental topic in theoretical ecology, as they govern population regulation, species coexistence, and ecosystem stability. Mathematical models provide a fundamental framework for understanding these interactions by revealing how nonlinear feedback mechanisms shape population persistence, extinction, and oscillatory dynamics [1, 2]. Over the past decades, predator–prey modeling has evolved continuously to incorporate biologically relevant mechanisms that improve the realism of population-level descriptions. A key modeling component is the functional response, which characterizes how predator consumption rates depend on prey density. Holling introduced several classes of functional responses to represent different feeding mechanisms [3]. Among these, the Holling type II functional response explicitly accounts for predator handling time and saturation effects, making it particularly suitable for modeling

*Corresponding author. E-mail: diansavitri@unesa.ac.id

Submitted: February 10, 2026 Reviewed: February 22, 2026 Accepted: March 12, 2026
DOI: https://doi.org/10.18860/cauchy.v11i1.41044

nonlinear predation processes. Consequently, this functional form has been widely adopted in studies addressing equilibrium stability, persistence, and oscillatory behavior in predator–prey systems [4–6]. Beyond predation, numerous biological factors have been incorporated into predator–prey models to better reflect empirical observations. These include migration [7, 8], refuge effects [9], disease dynamics [10, 11], and cannibalism [12]. Among these mechanisms, cannibalism, defined as the consumption of individuals of the same species, plays a significant role in population regulation and demographic structure [13–15]. Empirical evidence shows that cannibalism is widespread across taxa, including insects [16], amphibians [17], fish [18], mammals [19], and arthropods [20], indicating that it is a common ecological process rather than an exceptional phenomenon [21, 22]. In predator populations, cannibalism is frequently associated with stage structure due to size asymmetry and distinct energetic requirements between juvenile and adult individuals. Adult predators often prey upon juvenile conspecifics, generating stage-dependent cannibalistic interactions that affect recruitment, survival, and long-term population stability [23, 24]. Such interactions naturally motivate stage-structured modeling approaches, in which populations are divided into biologically meaningful classes to capture life stage-dependent processes. Stage-structured cannibalism models have been studied in single-species settings, where interactions between juvenile and adult stages significantly influence population dynamics [25]. Extending this framework to predator–prey systems, Zhang et al. [26] proposed a three-dimensional model in which the predator population is structured into juvenile and adult classes, allowing cannibalism to emerge explicitly. However, their formulation utilizes a linear Holling type I functional response, which fails to account for predator saturation effects during prey consumption and cannibalism. In a complementary direction, Rayungsari et al. [27] investigated predator–prey dynamics with predator cannibalism using a nonlinear Holling type II functional response, yet their framework is restricted to a two-dimensional system that lacks an explicit maturation process from juvenile to adult stages. Consequently, a gap remains in understanding how the synergistic effects of saturation, stage-dependent interactions, and maturation delay jointly influence population oscillations. From a dynamical systems perspective, nonlinear predator–prey models often exhibit qualitative transitions in behavior as parameters vary, including the emergence of sustained population oscillations through Hopf bifurcation. Hopf bifurcation provides a rigorous mathematical mechanism for explaining recurrent population cycles, whereby the loss of stability of an equilibrium gives rise to periodic solutions. Such phenomena are well documented in predator–prey systems with nonlinear functional responses and are particularly pronounced in models incorporating cannibalism, where additional nonlinear feedback can destabilize equilibria and generate oscillatory dynamics [12, 28]. Motivated by these considerations, the present study formulates and analyzes a modified three-dimensional predator–prey model. This model explicitly incorporates predator stage structure and maturation rates [26], while both prey predation and cannibalistic interactions follow Holling type II functional responses [27]. The primary objective is to investigate the qualitative dynamics of the model, with a specific focus on how adult predation intensity, maturation rates, and cannibalism levels jointly drive equilibrium stability and the emergence of Hopf bifurcations. By combining analytical Routh–Hurwitz criteria with numerical continuation in MatCont and Python-based simulations, this work aims to clarify how stage-dependent cannibalism, maturation, and nonlinear predation jointly shape population dynamics. The remainder of this paper is organized as follows. Section 2 describes the research methodology. Section 3 presents the results and discussion, covering the model formulation and its biological interpretation, existence and stability analysis, numerical simulations, and investigations of Hopf bifurcation. Finally, Section 4 provides the concluding remarks.

2. Research Methodology

The dynamical analysis of the proposed predator–prey model is conducted through a structured computational framework. This section specifies the numerical protocols and software configura-

tions used to ensure the reproducibility of the results, addressing the requirements for precise simulation settings.

2.1. Numerical Integration and Stability Verification

To validate the analytical local stability of the equilibrium points and visualize the phase portraits, numerical simulations are performed using the `SciPy` library in Python (Version 3.9+).

- Solver and Algorithm: The system is integrated using the `solve_ivp` function with the RK45 (explicit Runge–Kutta of order 5(4)) algorithm.
- Simulation Settings: Relative and absolute error tolerances are set to 10^{-8} and 10^{-10}, respectively. Simulations are conducted over a time horizon of $t \in [0, 600]$ with a maximum step size of $h_{max} = 0.4$ to ensure accurate capture of transient dynamics and convergence behavior.
- Initial Conditions: Multiple initial conditions are selected in the neighborhood of the coexistence equilibrium $E_2 = (x^*, y^*, z^*)$ to confirm local asymptotic stability. These include combinations of perturbations such as $(1.20x^*, 0.80y^*, 0.80z^*)$, $(0.70x^*, 1.40y^*, 1.10z^*)$, and $(1.10x^*, 1.10y^*, 0.60z^*)$.

2.2. Bifurcation Analysis and Continuation Protocols

The detection of Hopf and Branch Point (BP) singularities is executed using the MatCont (Version 7.3) continuation package within the MATLAB environment.

- Continuation Algorithm: Equilibrium curves are tracked using the Moore–Penrose prediction–correction algorithm. The continuation process starts from the established coexistence equilibrium and follows changes in key parameters: the adult predation rate (m_1), maturation rate (m), and maximum cannibalism rate (m_2).
- Step-Size and Tolerance: Adaptive step-size control is configured with `MaxStepsize` = 0.1, `MinStepsize` = 10^{-5}, and `InitStepsize` = 0.01. The singularity detection tolerance (`TestTolerance`) is set to 10^{-5}, `FunTolerance` = 10^{-6}, and `VarTolerance` = 10^{-6}.
- Corrector and Singularity Detection: The Newton–Raphson corrector iteration is restricted to a maximum of `MaxNewtonIters` = 3 and `MaxCorrIters` = 10. For singularity detection, the maximum number of test iterations is set to `MaxTestIters` = 10. The system employs an adaptation parameter `Adapt` = 3 to refine the mesh during continuation.
- Continuation Control and Stopping Criteria: The equilibrium curves are tracked using the Moore–Penrose algorithm with a `TSearchOrder` enabled for optimal branch tracking. The continuation process is programmed to terminate once the number of computed points reaches `MaxNumPoints` = 300. Additionally, the `CheckClosed` parameter is set to 50 to detect potential closed orbits or loops. Numerical derivatives are calculated using a `Jacobian Increment` of 10^{-5}.
- Hopf Classification: At each identified Hopf point, the First Lyapunov Coefficient (L_1) is calculated. This coefficient is used to classify the bifurcation as either supercritical ($L_1 < 0$) or subcritical ($L_1 > 0$), thereby determining the stability of the emerging periodic orbits.

2.3. Parameter Selection and Data Availability

The baseline parameter set provided in Table 1 is derived from a combination of established ecological literature and numerical assumptions. Parameters representing biological growth and interaction rates are selected based on various reported values in predator–prey studies to ensure ecological relevance. Conversely, specific parameters including n_1, m_2, and m are established through numerical assumptions to satisfy the analytical conditions for the existence and local stability of the positive coexistence equilibrium. The Python scripts for numerical simulations and the MatCont session files used in this study are hosted in a GitHub repository.

3. Results and Discussion

This section presents the main analytical and numerical findings of the proposed model and discusses their biological implications. We begin by formulating the mathematical system and identifying its equilibrium points, then examine the corresponding local stability conditions. The discussion is subsequently extended through numerical simulations and bifurcation analysis to illustrate how predation, maturation, and cannibalism shape the qualitative dynamics of the stage-structured predator–prey system.

3.1. Mathematical Model

In this article, the mathematical model is formulated based on the following assumptions:

1. The prey population $x(t)$ grows logistically with intrinsic growth rate r and carrying capacity K, and is reduced through predation by adult predators following a Holling type II functional response, where m_1 denotes the maximum predation rate of adult predators on prey and n_1 represents the half-saturation constant measuring predator saturation at high prey density.
2. The predator population is divided into juvenile predators $y(t)$ and adult predators $z(t)$. Juvenile predators do not consume prey and are produced by adult predators at a constant per capita rate b.
3. Juvenile predators mature into adult predators at a constant per capita rate m, while adult predators prey upon juvenile predators through intraspecific cannibalism described by a Holling type II functional response, where m_2 denotes the maximum cannibalism rate and n_2 is the corresponding half-saturation constant.
4. The growth of the adult predator population results from the consumption of prey and juvenile predators with constant conversion efficiencies e_1 and e_2, respectively, whereas juvenile and adult predators experience natural mortality at rates d_1 and d_2.
5. The system evolves in a closed and homogeneous environment with no migration and constant environmental conditions.

From the assumptions stated above, the dynamics of the system are governed by the following set of ordinary differential equations:

$$\begin{aligned}
\frac{dx}{dt} &= rx\left(1-\frac{x}{K}\right) - \frac{m_1 xz}{n_1+x} \\
\frac{dy}{dt} &= bz - \frac{m_2 yz}{n_2+y} - my - d_1 y \\
\frac{dz}{dt} &= e_1\frac{m_1 xz}{n_1+x} + e_2\frac{m_2 yz}{n_2+y} + my - d_2 z
\end{aligned} \tag{1}$$

where $x(t)$, $y(t)$, and $z(t)$ denote the densities of prey, juvenile predators, and adult predators at time t, respectively, with initial conditions $x(0) > 0$, $y(0) > 0$, and $z(0) > 0$

3.2. Existence and Stability Analysis of Equilibrium Points

In this section, the equilibrium points of system (1) are obtained by solving

$$\begin{aligned}
rx\left(1-\frac{x}{K}\right) - \frac{m_1 xz}{n_1+x} &= 0 \\
bz - \frac{m_2 yz}{n_2+y} - my - d_1 y &= 0 \\
e_1\frac{m_1 xz}{n_1+x} + e_2\frac{m_2 yz}{n_2+y} + my - d_2 z &= 0
\end{aligned} \tag{2}$$

From system (2), we obtain the following equilibrium points, i.e:

1. The trivial equilibrium point
$$E_0 = (0, 0, 0)$$
which always exists and corresponds to the extinction of all populations.
2. The prey-only equilibrium point
$$E_1 = (K, 0, 0)$$
which always exists and represents the survival of the prey population in the absence of predators.
3. The coexistence equilibrium point
$$E_2 = (x^*, y^*, z^*)$$
where $x^* > 0$, $y^* > 0$, and $z^* > 0$ satisfy system (2). The coexistence equilibrium of system (1) is denoted by
$$E_2 = (x^*, y^*, z^*) \in \mathbb{R}^3_+$$
From the prey equation, the adult predator density is given by
$$z^* = \frac{r(n_1 + x^*)}{m_1}\left(1 - \frac{x^*}{K}\right), \qquad 0 < x^* < K \tag{3}$$
From the juvenile predator equation, y^* satisfies the quadratic equation
$$(m + d_1)y^2 + \left[(m + d_1)n_2 + (m_2 - b)z^*\right]y - bn_2z^* = 0 \tag{4}$$
which admits a unique positive solution
$$y^* = \frac{(b - m_2)z^* - (m + d_1)n_2 + \sqrt{\Delta}}{2(m + d_1)} \tag{5}$$
where
$$\Delta = \left[(b - m_2)z^* - (m + d_1)n_2\right]^2 + 4(m + d_1)bn_2z^*$$
Substituting Eq. (3) and Eq. (5) into the predator equation yields a scalar equation
$$\Phi(x^*) = 0 \tag{6}$$
which determines $x^* \in (0, K)$.
Consequently, the coexistence equilibrium can be written as
$$E_2 = (x^*,\ y^*,\ z^*)$$
where x^* satisfies Eq. (6), and y^* and z^* are given by Eq. (5) and Eq. (3), respectively. The coexistence equilibrium E_2 exists provided that the following conditions are satisfied:

$$\begin{aligned}
&\text{(H1) } r > 0, \quad K > 0,\\
&\text{(H2) } \frac{e_1m_1K}{n_1 + K} + \frac{mb}{m + d_1} > d_2,\\
&\text{(H3) } x^* < K.
\end{aligned}$$

Condition (H2) ensures that the predator population can invade the system when the prey is at its carrying capacity, while (H3) guarantees that the equilibrium point lies within the biologically feasible range.

Now, study the local stability of the dynamic system (1) around each of equilibrium points. The Jacobian matrix of the system (1) is determined as:

$$J(x,y,z) = \begin{pmatrix} r\left(1-\dfrac{2x}{K}\right) - \dfrac{m_1 z n_1}{(n_1+x)^2} & 0 & -\dfrac{m_1 x}{n_1+x} \\ 0 & -\dfrac{m_2 z n_2}{(n_2+y)^2} - (m+d_1) & b - \dfrac{m_2 y}{n_2+y} \\ \dfrac{e_1 m_1 z n_1}{(n_1+x)^2} & \dfrac{e_2 m_2 z n_2}{(n_2+y)^2} + m & \dfrac{e_1 m_1 x}{n_1+x} + \dfrac{e_2 m_2 y}{n_2+y} - d_2 \end{pmatrix}$$

By evaluating the Jacobian matrix at each equilibrium point, the local stability properties of the equilibria are obtained as follows.

Theorem 1. *The trivial equilibrium point $E_0 = (0,0,0)$ is always unstable.*

Proof. The Jacobian matrix evaluated at E_0 is given by

$$J(E_0) = \begin{pmatrix} r & 0 & 0 \\ 0 & -(m+d_1) & b \\ 0 & m & -d_2 \end{pmatrix}$$

The characteristic equation is

$$(\lambda - r)\left[\lambda^2 + (m+d_1+d_2)\lambda + d_2(m+d_1) - bm\right] = 0$$

Thus, the first eigenvalue of the Jacobian matrix $J(E_0)$ is $\lambda_1 = r > 0$, while the remaining eigenvalues λ_2 and λ_3 are determined by the quadratic factor. Since at least one eigenvalue has a positive real part, the equilibrium point E_0 is unstable. □

Theorem 2. *If*

$$m + d_1 > 0 \quad \text{and} \quad d_2 > \frac{e_1 m_1 K}{n_1 + K}$$

then the prey-only equilibrium point E_1 of the system is locally asymptotically stable.

Proof. The Jacobian matrix evaluated in equilibrium point E_1 is given by

$$J(E_1) = \begin{pmatrix} -r & 0 & -\dfrac{m_1 K}{n_1+K} \\ 0 & -(m+d_1) & b \\ 0 & 0 & \dfrac{e_1 m_1 K}{n_1+K} - d_2 \end{pmatrix}$$

The eigenvalues associated with the Jacobian matrix $J(E_1)$ are derived as

$$\lambda_1 = -r, \quad \lambda_2 = -(m+d_1), \quad \lambda_3 = \frac{e_1 m_1 K}{n_1+K} - d_2$$

Since $\lambda_1 < 0$ and $\lambda_2 < 0$. the stability of E_1 depends on $\lambda_3 < 0$. If

$$d_2 > \frac{e_1 m_1 K}{n_1 + K}$$

then all eigenvalues of $J(E_1)$ have negative real parts, ensuring local asymptotic stability. □

Theorem 3. *The positive coexistence equilibrium E_2 of system (1) is locally asymptotically stable if the coefficients a_1, a_2, and a_3 of the characteristic polynomial $\lambda^3+a_1\lambda^2+a_2\lambda+a_3 = 0$ satisfy the Routh–Hurwitz conditions:*

$$a_1 > 0, \quad a_3 > 0, \quad \text{and} \quad a_1 a_2 > a_3$$

where these conditions are specifically determined by the interaction rates of prey predation, predator maturation, and stage-dependent cannibalism.

Proof. The Jacobian matrix of the system evaluated at the equilibrium point E_2 is given by:

$$J(E_2) = \begin{pmatrix} J_{11} & J_{12} & J_{13} \\ J_{21} & J_{22} & J_{23} \\ J_{31} & J_{32} & J_{33} \end{pmatrix}$$

where the explicit entries are defined as follows:

$$\begin{aligned}
J_{11} &= r\left(1 - \frac{2x^*}{K}\right) - \frac{m_1 z^* n_1}{(n_1 + x^*)^2} \\
J_{12} &= 0 \\
J_{13} &= -\frac{m_1 x^*}{n_1 + x^*} \\
J_{21} &= 0 \\
J_{22} &= -\frac{m_2 z^* n_2}{(n_2 + y^*)^2} - (m + d_1) \\
J_{23} &= b - \frac{m_2 y^*}{n_2 + y^*} \\
J_{31} &= \frac{e_1 m_1 z^* n_1}{(n_1 + x^*)^2} \\
J_{32} &= \frac{e_2 m_2 z^* n_2}{(n_2 + y^*)^2} + m \\
J_{33} &= \frac{e_1 m_1 x^*}{n_1 + x^*} + \frac{e_2 m_2 y^*}{n_2 + y^*} - d_2
\end{aligned}$$

By utilizing the equilibrium condition $r(1 - x^*/K) = \frac{m_1 z^*}{n_1 + x^*}$, the entry J_{11} can be simplified to $J_{11} = -\frac{rx^*}{K} + \frac{m_1 x^* z^*}{(n_1+x^*)^2}$, which highlights the stabilizing effect of intraspecific competition. Since $J_{12} = 0$ and $J_{21} = 0$, the characteristic equation $\det(\lambda I - J(E_2)) = 0$ expands to the following polynomial:

$$\lambda^3 + a_1\lambda^2 + a_2\lambda + a_3 = 0$$

The model-specific coefficients are explicitly derived as:

$$\begin{aligned}
a_1 &= -(J_{11} + J_{22} + J_{33}) \\
a_2 &= J_{11}J_{22} + J_{11}J_{33} + J_{22}J_{33} - J_{13}J_{31} - J_{23}J_{32} \\
a_3 &= -J_{11}(J_{22}J_{33} - J_{23}J_{32}) + J_{13}J_{22}J_{31}
\end{aligned}$$

According to the Routh–Hurwitz criteria, the local asymptotic stability of E_2 is ensured if $a_1 > 0$, $a_3 > 0$, and $a_1 a_2 > a_3$. Structurally, the term $-J_{13}J_{31} > 0$ represents the stabilizing negative feedback of the prey–adult predator interaction. Conversely, the term $-J_{23}J_{32}$ represents the coupling between juvenile and adult stages, which can be destabilizing if

maturation and cannibalism rates are sufficiently high. Specifically, $a_3 > 0$ is guaranteed when the stabilization from predation and diagonal damping dominates the stage-structured interactions. Under these parameter-specific conditions, E_2 is locally asymptotically stable. □

3.3. Numerical Simulation

Numerical simulations are conducted to illustrate the dynamical behavior of model (1). We utilize the parameter set listed in Table 1, which is selected to ensure the existence and local stability of the positive coexistence equilibrium E_2. While some theoretical conditions for coexistence depend on complex nonlinear thresholds, the chosen values satisfy the criteria for a biologically feasible steady state where all populations persist. Specifically, the interplay between the maturation rate ($m = 0.25$) and birth rate of juvenile predators ($b = 0.4$) is balanced by the supplementary energetic gains from cannibalism ($e_2 = 0.15$) and prey consumption ($e_1 = 0.2$), allowing for a stable coexistence at $E_2 = (59.9078, 23.9092, 56.0552)$.

Table 1: Parameter Values for Numerical Simulation

Parameter	Description	Value	Reference
r	Intrinsic growth rate of prey	0.8	[29]
K	Carrying capacity of prey	100	[30, 31]
m_1	Maximum consumption rate of adult predators on prey	0.4	[27]
n_1	Half-saturation constant for prey consumption	10	Assumed
m_2	Maximum cannibalism rate of adults on juvenile predators	0.2	Assumed
n_2	Half-saturation constant for cannibalism	5	[32]
e_1	Conversion efficiency rate from prey to adult predators	0.2	[27]
e_2	Conversion efficiency rate from juvenile predators to adults	0.15	[33]
b	Birth rate of juvenile predators produced by adults	0.4	[34]
m	Maturation rate from juvenile to adult predators	0.25	Assumed
d_1	Natural mortality rate of juvenile predators	0.3	[33]
d_2	Natural mortality rate of adult predators	0.2	[33]

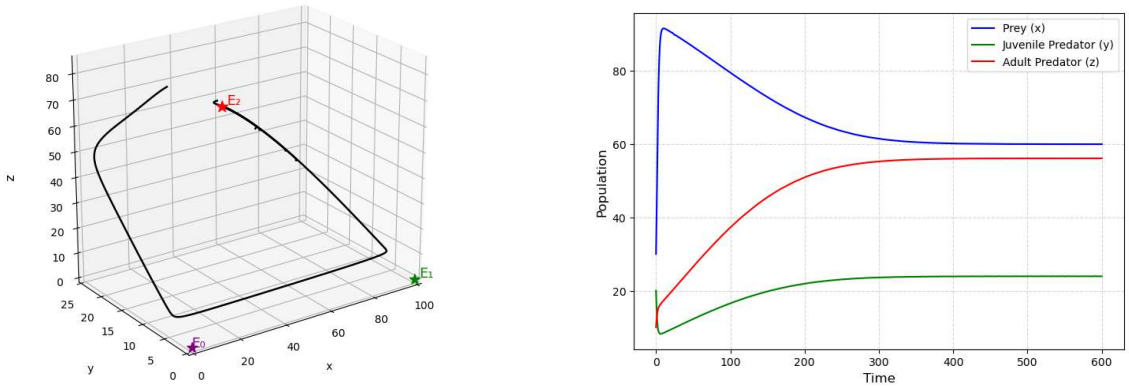

(a) Phase portrait showing convergence to E_2 **(b)** Time series evolution of the populations

Fig. 1: Numerical simulations of the model for parameter set Table 1. (a) Trajectories contracting toward the stable equilibrium E_2, and (b) convergence of state variables to their respective steady states

The numerical integration is performed using the `SciPy` library in Python, specifically employing the `solve_ivp` function with the RK45 (explicit Runge–Kutta of order 5(4)) algorithm. To ensure high numerical precision and reproducibility, we set the relative and absolute error tolerances to 10^{-8} and 10^{-10}, respectively, over a time horizon of $T \in [0, 600]$ units with a maximum step size of $h_{max} = 0.4$.

The numerical results, depicted in Fig. 1, illustrate the trajectories starting from multiple initial conditions to verify the robustness of the local asymptotic stability. As specified in the methodology, we consider three distinct initial states derived from explicit perturbations of the equilibrium point E_2 as follows:

- $P_1 = (1.20x^*, 0.80y^*, 0.80z^*) = (71.8894, 19.1274, 44.8442)$,
- $P_2 = (0.70x^*, 1.40y^*, 1.10z^*) = (41.9355, 33.4729, 61.6607)$,
- $P_3 = (1.10x^*, 1.10y^*, 0.60z^*) = (65.8986, 26.3001, 33.6331)$.

The three-dimensional phase portrait in Fig. 1a shows that solution trajectories starting within the vicinity of the equilibrium are attracted toward the positive coexistence equilibrium $E_2 = (59.9078, 23.9092, 56.0552)$, indicating asymptotic convergence within the local neighborhood of the equilibrium. In addition, the time series in Fig. 1b illustrates the temporal evolution of the prey, juvenile predator, and adult predator populations, where all state variables exhibit decay of transient dynamics and approach constant steady-state values.

To verify these observations analytically, the eigenvalues of the Jacobian matrix $J(E_2)$ is computed, yielding a spectrum given by $\{\lambda_1, \lambda_2, \lambda_3\} = \{-0.1905, -0.0214, -0.7162\}$. Since all eigenvalues lie entirely in the open left half of the complex plane ($\mathrm{Re}(\lambda_i) < 0$), the coexistence equilibrium E_2 is confirmed to be locally asymptotically stable. This spectral configuration is in full agreement with the qualitative behavior observed in the simulations.

Conceptually, our results extend the findings of Zhang et al. [26] and Rayungsari et al. [27] by examining the interplay between saturation and stage transitions. Unlike the linear maturation effects reported in [26], the integration of a Holling type II functional response for both predation and cannibalism introduces a saturation-induced damping that shifts the stability thresholds. Furthermore, compared to the two-dimensional framework in [27], our three-dimensional approach reveals that the maturation rate m acts as a critical stabilization parameter; high maturation rates prevent the rapid predator population crashes that often destabilize simpler systems. These simulations demonstrate that while some parameters are based on numerical assumptions, the synergy between stage structure and nonlinear cannibalism appears to provide a stabilizing effect for system (1) under the parameters investigated.

3.4. Hopf Bifurcation

In this section, we perform a detailed numerical investigation of the Hopf bifurcation using the continuation software MatCont (Version 7.3) within the MATLAB environment. These simulations aim to numerically investigate and to characterize the emergence and stability of periodic limit cycles. Specifically, we employ a Moore–Penrose continuation algorithm to track the equilibrium curve in the extended state-parameter spaces.

To ensure reproducibility and high-precision detection of singularities, the adaptive step-size control is configured with a `MaxStepsize` of 0.1, a `InitStepsize` of 0.01, a `MinStepsize` of 10^{-5}, a `TestTolerance` for Hopf points set to 10^{-5}, `FunTolerance` set to 10^{-6}, and `VarTolerance` set to 10^{-6}. The Newton–Raphson corrector iteration is restricted to a maximum of `MaxNewtonIters` $= 3$ and `MaxCorrIters` $= 10$. For singularity detection, the maximum number of test iterations is set to `MaxTestIters` $= 10$. The system employs an adaptation parameter `Adapt` $= 3$ to refine the mesh during continuation.

The continuation process is programmed to terminate once the number of computed points reaches `MaxNumPoints` $= 300$. Additionally, the `CheckClosed` parameter is set to 50 to detect potential closed orbits or loops. Numerical derivatives are calculated using a `Jacobian Increment` of 10^{-5}.

3.4.1. *The Impact of Adult Predation Intensity on Oscillatory Dynamics*

We first investigate the dynamical response of system (1) to variations in the parameter m_1, which represents the maximum consumption rate of adult predators on prey. Numerical

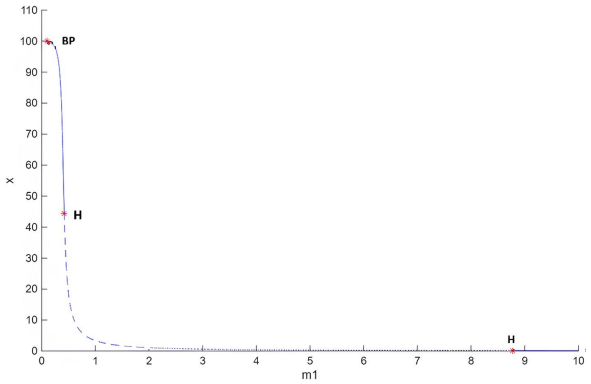

(a) Time series of $x(t)$ for m_1

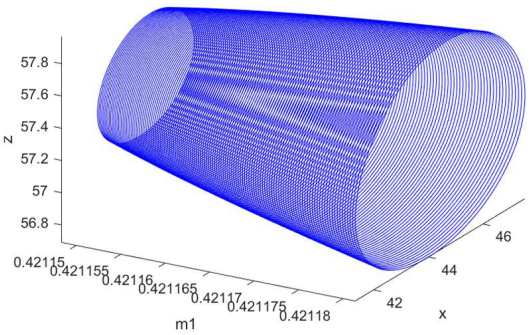

(b) Hopf bifurcation manifold for m_1

Fig. 2: Numerical bifurcation analysis for parameter m_1: (a) population time series in (m_1, x) and (b) bifurcation manifold in (m_1, x, z)-space

continuation reveals two distinct Hopf bifurcation points along the coexistence equilibrium branch, labeled H_1 and H_2. The first Hopf point is located at:

$$H_1 : (x, y, z, m_1) = (44.411994, 24.441966, 57.457628, 0.421132).$$

At H_1, the First Lyapunov Coefficient is calculated to be $L_1 \approx -8.430934 \times 10^{-5}$. Since $L_1 < 0$, the bifurcation is classified as supercritical, indicating the emergence of a stable branch of periodic orbits as the equilibrium point loses stability. The second Hopf point occurs at:

$$H_2 : (x, y, z, m_1) = (0.144764, 0.634049, 0.923798, 8.772544).$$

At H_2, the First Lyapunov Coefficient is calculated to be $L_1 \approx 4.256313 \times 10^{-3}$. Since $L_1 > 0$, the bifurcation is classified as subcritical, confirming the birth of an unstable branch of periodic orbits as the equilibrium point loses stability. As m_1 crosses these critical thresholds, a clear stability switch occurs. For $m_1 < 0.421132$, the coexistence equilibrium is locally asymptotically stable, represented by the solid blue line, acting as a sink. As m_1 increases beyond 0.421132, the equilibrium becomes unstable(indicated by the dashed blue line), giving rise to persistent periodic oscillations. These oscillations persist within the interval $0.421132 < m_1 < 8.772544$ This transition is consistent with the time series in Fig. 2a, where stable equilibrium give way to persistent limit cycles. The corresponding three-dimensional projection in the (m_1, x, z) space (Fig. 2b) highlights the geometric organization of the equilibrium branch and the associated stability changes induced by interspecific predation intensity.

Furthermore, a Branch Point (BP) is detected at:

$$BP : (x, y, z, m_1) = (100.00, 0.00, 0.00, 0.10).$$

The dynamical significance of this point lies in its role as a critical threshold where the coexistence equilibrium branch E_2 intersects the prey-only manifold $E_1(K, 0, 0)$. Biologically, the BP marks the transition point where the predator population can potentially invade the system, for $m_1 < 0.10$, the predator population cannot sustain itself and faces extinction, whereas for $m_1 > 0.10$, the predator can invade and settle into a locally stable coexistence state.

The presence of two Hopf points and a BP along the same continuation curve underscores the high sensitivity of system (1) to predation pressure. Unlike simpler models that exhibit monotonic stability, our quantitative diagnostics indicate that adult predation intensity creates a bounded instability window, where oscillations are sustained within a specific parameter range. This supercritical behavior suggests that the system transitions smoothly from a steady state to a stable oscillatory regime, emphasizing the role of stage structure in modulating ecological stability.

3.4.2. *The Impact of Maturation Rate on Stage-Structured Oscillatory Dynamics*

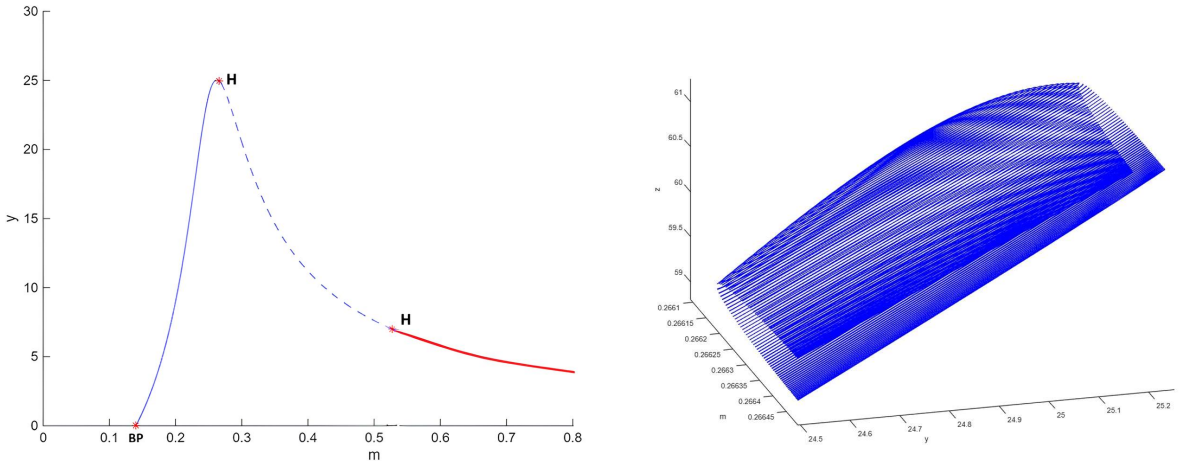

(a) Time series of $y(t)$ for m **(b)** Hopf bifurcation manifold for m

Fig. 3: Numerical bifurcation analysis for parameter m: (a) population time series in (m, y) and (b) bifurcation manifold in (m, y, z)-space

We next analyze system (1) with respect to the maturation parameter m, which governs the transition rate from juvenile to adult predators and controls the internal population flux within the predator population.

The first Hopf point is detected at:

$$H_1 : (x, y, z, m) = (44.398902, 24.939956, 60.492774, 0.266121).$$

At this point, the First Lyapunov Coefficient is calculated as $L_1 \approx -7.905271 \times 10^{-5}$. Since $L_1 < 0$, the bifurcation is classified as supercritical, suggesting the emergence of a stable branch of periodic orbits as the equilibrium point loses stability. The second Hopf point occurs at:

$$H_2 : (x, y, z, m) = (0.250470, 7.004695, 20.449591, 0.527072),$$

with a corresponding First Lyapunov Coefficient of $L_1 \approx -1.267874 \times 10^{-4}$, which also indicates a supercritical transition.

The variation in m is associated with a stability switch, defining a bounded window of oscillatory dynamics, as illustrated in the bifurcation diagram in Fig. 3a. For $m < 0.266121$, the coexistence equilibrium is locally asymptotically stable, represented by the solid blue line. As m increases beyond H_1, the steady state becomes unstable (indicated by the dashed blue line), giving rise to sustained periodic oscillations as shown in the time series (Fig. 3a). These oscillations persist within the interval $0.266121 < m < 0.527072$.

The evolution of these periodic dynamics is further characterized by the three-dimensional solution manifold in the (y, z, m) space, as illustrated in Fig. 3b. This manifold represents the family of stable limit cycles bifurcating from H_1 as the maturation rate varies. The geometric structure, appearing as a dense cylindrical surface, highlights the continuous variation in the oscillation amplitudes of both juvenile (y) and adult (z) predator populations. The structure of this manifold suggests that the transition from a stable equilibrium to a periodic regime is non-abrupt, consistent with the supercritical nature of the detected Hopf points.

Beyond the second Hopf point H_2, the equilibrium branch briefly regains stability before reaching the boundary of the biologically feasible state space. As shown in Fig. 3a, the continuation curve transitions to a red color near $m \approx 0.537$, signifying that the equilibrium values are no longer ecologically feasible. Although a Branch Point (BP) is detected at $m \approx 0.537256$ with coordinates $(x \approx -0.000000, y \approx 6.801606, z \approx 20.000000)$, the prey population x effectively becomes negative. Similarly, a BP detected at $m \approx 0.140000$ involves a negative adult predator

population ($z \approx -0.000000$). These points and the subsequent red segments are disregarded in the biological analysis, as they represent mathematical continuations where at least one species faces extinction. Specifically, the transition to the red line marks the termination of the coexistence manifold, indicating that excessively high maturation rates lead to prey extinction within the model.

Biologically, these results highlight that maturation acts as a key internal timescale capable of destabilizing steady coexistence. The negative First Lyapunov coefficients suggest that the emerging oscillations are stable. However, the system's viability is restricted to a finite window of maturation rates, beyond which the nonlinear feedback mechanisms fail to maintain a three-species coexistence.

3.4.3. *The Impact of Cannibalism Intensity on Hopf Bifurcation and Periodic Dynamics*

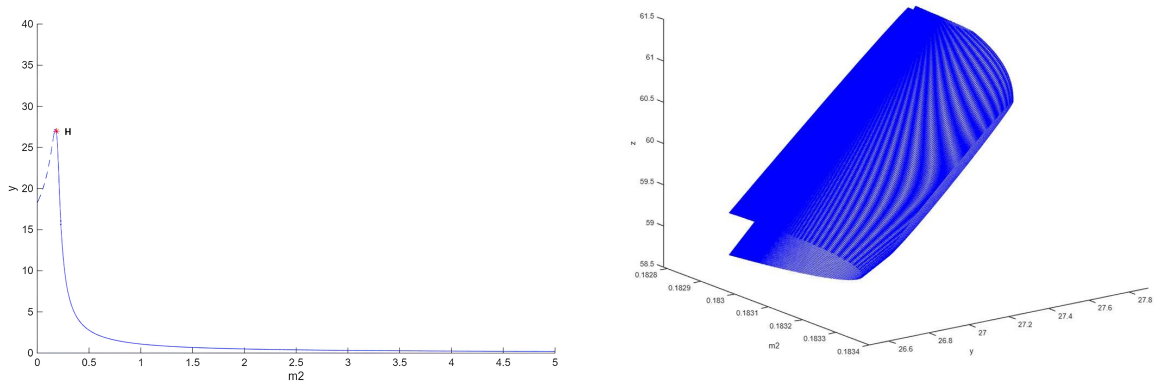

(a) Time series of $y(t)$ for m_2 **(b)** Hopf bifurcation manifold for m_2

Fig. 4: Numerical bifurcation analysis for parameter m_2: (a) population time series in (m_2, y) and (b) bifurcation manifold in (m_2, y, z)-space

Finally, we examine the role of the cannibalism parameter m_2, which represents the maximum cannibalism rate of adult predators on juvenile predators and thus quantifies the intensity of intraspecific predation. Numerical continuation of equilibria in the extended state-parameter space (x, y, z, m_2) reveals a Hopf bifurcation point along the coexistence equilibrium branch, labeled H, located at:

$$H : (x, y, z, m_2) = (44.478173, 26.973268, 60.494554, 0.183455).$$

At this critical point, the First Lyapunov Coefficient is calculated to be $L_1 \approx -8.816416 \times 10^{-5}$. Since $L_1 < 0$, the bifurcation is classified as supercritical, suggesting the emergence of a stable branch of periodic orbits as the coexistence equilibrium loses stability.

The variation in m_2 induces a distinct stability switch in the system's qualitative behavior. For $m_2 < 0.183455$, the coexistence equilibrium is unstable(indicated by the dashed blue line), giving rise to sustained periodic oscillations. As the cannibalism rate increases beyond this threshold, the steady state becomes locally asymptotically stable(represented by the solid blue line), acting as a sink for nearby trajectories. This transition is consistent with the time series in Fig. 4a, where the decay of transient dynamics gives way to persistent limit cycles.

The continuation of periodic solutions originating from H manifests as a curved, half-loop-like surface in the (y, z, m_2) space, as shown in Fig. 4b. This geometry reflects the biologically admissible branch of periodic solutions parameterized by m_2. For each fixed value of m_2 within the oscillatory regime, the dynamics in the (y, z) phase plane consist of a closed periodic orbit, while the projection into the (y, z, m_2) space captures how the amplitude and position of these oscillations evolve with increasing cannibalism intensity.

Biologically, these results demonstrate that cannibalism introduces a strong nonlinear intraspecific feedback mechanism. While cannibalism is often viewed as a regulatory process,

our quantitative diagnostics show that sufficiently high cannibalistic pressure can destabilize population balance and induce sustained oscillations through a supercritical Hopf bifurcation. This highlights the dual role of cannibalism as both a survival strategy and a driver of complex temporal dynamics in stage-structured systems.

4. Conclusion

This study investigated the nonlinear dynamics of a three-dimensional predator–prey model incorporating a Holling type II functional response, predator stage structure, and cannibalism. The primary objective was to determine how maturation, adult predation, and cannibalism rates jointly govern equilibrium stability and the emergence of periodic oscillations. Numerical simulations, performed using the Python `RK45` solver with high-precision tolerances, demonstrate that trajectories from within the local neighborhood of the equilibrium converge asymptotically toward the positive coexistence equilibrium $E_2 = (59.9078, 23.9092, 56.0552)$. This local stability is numerically verified by the eigenvalues of the Jacobian matrix $J(E_2)$, which are found to be $\{-0.1905, -0.0214, -0.7162\}$. Since all eigenvalues have negative real parts, E_2 is characterized as a stable node for the investigated parameter set.

Numerical continuation reveals that this stable regime is bounded by multiple Hopf bifurcation thresholds associated with distinct biological mechanisms. For the adult predation parameter m_1, an instability window exists between $m_1 \approx 0.4211$ and $m_1 \approx 8.7725$. While the first Hopf point is supercritical ($L_1 < 0$), indicating the birth of stable periodic orbits, the second point at $m_1 \approx 8.7725$ is identified as subcritical ($L_1 > 0$). Similarly, variations in the maturation rate m induce supercritical Hopf bifurcations ($L_1 < 0$) at $m \approx 0.2661$ and $m \approx 0.5271$. Furthermore, the detection of a Branch Point (BP) at $m_1 = 0.10$ identifies a critical invasion threshold, below which the predator population cannot sustain itself. These numerical findings remain consistent with the analytical coexistence conditions satisfied by the chosen parameter set.

The analysis of the cannibalism parameter m_2 identifies a supercritical Hopf bifurcation at $m_2 \approx 0.1835$. The resulting periodic solution manifold illustrates that while cannibalism is often a regulatory mechanism, it introduces a nonlinear feedback capable of destabilizing the population balance once its intensity exceeds a specific threshold. Overall, the results demonstrate that oscillatory dynamics in the proposed stage-structured system arise through multiple, quantitatively distinct Hopf bifurcation mechanisms, involving both stable and unstable periodic regimes.

Despite the comprehensive nature of these findings, this study is subject to certain limitations. The analysis relies on numerical bifurcation methods and assumed parameter values for specific interaction rates, as explicit analytical Hopf conditions for the three-dimensional system remain to be derived. Future work may address these by developing formal analytical proofs for the bifurcation boundaries or extending the framework to incorporate environmental stochasticity and time delays to further explore the robustness of the observed oscillatory regimes.

CRediT Authorship Contribution Statement

Sela Tri Indah Sari: Conceptualization, Methodology, Software, Formal Analysis, Investigation, Writing–Original Draft, Visualization. **Dian Savitri:** Conceptualization, Methodology, Validation, Writing–Review & Editing, Visualization, Supervision.

Declaration of Generative AI and AI-assisted technologies

During the preparation of this study, the authors additionally utilized ChatGPT to help with structural refinement and preliminary drafting, while Grammarly was used to improve grammatical accuracy and sentence structure. The writers accept full responsibility for the publication's content and have reviewed and amended it as necessary.

Declaration of Competing Interest

The authors declare no competing interests.

Funding and Acknowledgments

The authors would like to express their sincere gratitude to their supervisor for the invaluable guidance, constant encouragement, and insightful suggestions throughout the development of this study. Special thanks are also extended to all colleagues and individuals who provided technical assistance and support during the completion of this manuscript.

Data and Code Availability

The data and code supporting the findings of this study are publicly available. The Python scripts for numerical simulations and MatCont session files for bifurcation analysis can be accessed at the following GitHub[1] repository.

References

[1] A J Lotka. *Elements of Mathematical Biology*. Publications, 1956.

[2] Vito Volterra. "Fluctuations in The Abundance of a Species Considered Mathematically". In: *Nature* 118.2972 (1926), pp. 558–560.

[3] C. S. Holling. "Some Characteristics of Simple Types of Predation and Parasitism". In: *The Canadian Entomologist* 91.7 (1959), pp. 385–398. DOI: 10.4039/Ent91385-7.

[4] Shuangte Wang et al. "The Dynamical Behavior of a Predator-Prey System with Holling Type II Functional Response and Allee Effect". In: *Applied Mathematics* 11.05 (2020), pp. 1–19. DOI: 10.4236/am.2020.115029.

[5] Lazarus Kalvein Beay et al. "Hopf Bifurcation and Stability Analysis of The Rosenzweig–MacArthur Predator–Prey Model with Stage-Structure in Prey". In: *Mathematical Biosciences and Engineering* 17.4 (2020), pp. 4080–4097. DOI: 10.3934/mbe.2020226.

[6] Salima Helali, Dorsaf Laribi, and Haifa Ben Fredj. "Two-Prey Predator Model with Holling Type-II Functional Response and Multiple Delays: Hopf–Bifurcation Analysis, Parameters Estimation, and Capture Prediction". In: *Journal of Applied Mathematics and Computing* 71 (2025), pp. 7691–7724. DOI: 10.1007/s12190-025-02544-7.

[7] Xiangjun Dai et al. "Survival Analysis of a Predator–Prey Model with Seasonal Migration of Prey Populations between Breeding and Non-Breeding Regions". In: *Mathematics* 11.18 (2023). DOI: 10.3390/math11183838.

[8] Érika Diz-Pita. "Global Dynamics of a Predator-Prey System with Immigration in Both Species". In: *Electronic Research Archive* 32.2 (2024), pp. 762–778. DOI: 10.3934/era.2024036.

[9] Fitri Nur Azizah et al. "The Effect of Refugia on Prey-Predator Model with Parasite Infection". In: *International Journal of Applied Mathematics, Sciences, and Technology for National Defense* 2.2 (2024). DOI: 10.58524/app.sci.def.v2i2.423.

[10] Jingen Yang et al. "Spatiotemporal Dynamics of a Predator–Prey Model with Harvest and Disease in Prey". In: *Mathematics* 13.15 (2025). DOI: 10.3390/math13152474.

[1] https://github.com/Selaindah/A-Stage-Structured-Predator--Prey-Model-with-Holling-Type-II-Functional-Response-and-Cannibalism

[11] Nada A. Almuallem, Hasanur Mollah, and Sahabuddin Sarwardi. "A study of a Prey-Predator Model with Disease in Predator Including Gestation Delay, Dreatment and Linear Harvesting of Predator Species". In: *AIMS Mathematics* 10.6 (2025), pp. 14657–14698. DOI: 10.3934/math.2025660.

[12] Daifeng Duan et al. "The Dynamical Analysis of a Nonlocal Predator-Prey Model with Cannibalism". In: *European Journal of Applied Mathematics* 35.5 (2024), pp. 707–731. DOI: 10.1017/S0956792524000019.

[13] Gary A. Polis. "The Evolution and Dynamics of Intraspecific Predation". In: *Annual Review of Ecology and Systematics* 12 (1981), pp. 225–251. DOI: 10.1146/annurev.es.12.110181.001301.

[14] Qifa Lin et al. "Global attractivity of Leslie–Gower predator–prey Model Incorporating Prey Cannibalism". In: *Advances in Continuous and Discrete Models* 2020 (2020). DOI: 10.1186/s13662-020-02609-w.

[15] P. Mishra, S.N. Raw, and B. Tiwari. "On a Cannibalistic Predator–Prey Model with Prey Defense and Diffusion". In: *Applied Mathematical Modelling* 90 (2021), pp. 165–190. DOI: 10.1016/j.apm.2020.08.060.

[16] Francisco J. Fernández et al. "Do Development and Diet Determine the Degree of Cannibalism in Insects? To Eat or Not to Eat Conspecifics". In: *Insects* 11.4 (2020), p. 242. DOI: 10.3390/insects11040242.

[17] Erica L. Wildy and Matthew R. Whiles. "Cannibalism and Intraguild Predation Among Larval Amphibians Under Natural Conditions". In: *Ecology* 102.5 (2021), e03320. DOI: 10.1002/ecy.3320.

[18] Carlos A. Sepúlveda-Quiroz et al. "Tryptophan Reduces Intracohort Cannibalism Behavior in Tropical Gar (Atractosteus tropicus) Larvae". In: *Fishes* 9.1 (2024), p. 40. DOI: 10.3390/fishes9010040.

[19] Luis A. Ebensperger, Lynne D. Hayes, and Javier Ramírez-Estrada. "Sex-Specific Variation in Filial Cannibalism Among Mammals". In: *Biological Reviews* 95.6 (2020), pp. 1559–1575. DOI: 10.1111/brv.12640.

[20] Carlos S. Matos, Rafael S. Silva, and Daniel M. Oliveira. "First Record of Cannibalism in The Red-Finger Rubble Crab Eriphia Gonagra in a Natural Environment". In: *Journal of Crustacean Biology* 45.1 (2025), ruae005. DOI: 10.1093/jcbiol/ruae005.

[21] Lawrence R. Fox. "Cannibalism in Natural Populations". In: *Annual Review of Ecology and Systematics* 6 (1975), pp. 87–106. DOI: 10.1146/annurev.es.06.110175.000511.

[22] Mark A Elgar and Bernard J Crespi. *Cannibalism: Ecology and Evolution Among Diverse Taxa*. 361 p. Oxford, England; New York: Oxford University Press, 1992.

[23] J. Li and Z. Zhu. "Impact of Cannibalism on Dynamics of a Structured Predator–Prey System". In: *Applied Mathematical Modelling* 78 (2020), pp. 1–19. DOI: 10.1016/j.apm.2019.09.022.

[24] Y. Wei. "Stability Analysis of a Stage-Structure Predator–Prey System with Time Delay". In: *Axioms* 11.8 (2022), p. 421. DOI: 10.3390/axioms11080421.

[25] X. Li. "Global Analysis of a Juvenile-Adult Model for Cannibalistic Interactions". In: *International Journal of Biomathematics* 14.1 (2021), p. 2150045. DOI: 10.1142/S1793524521500455.

[26] Fengqin Zhang, Yuming Chen, and Jianquan Li. "Dynamical Analysis of a Stage-Structured Predator-Prey Model with Cannibalism". In: *Mathematical Biosciences* 307 (2019), pp. 33–41. DOI: 10.1016/j.mbs.2018.11.004.

[27] Maya Rayungsari et al. “Dynamical Analysis of a Predator-Prey Model Incorporating Predator Cannibalism and Refuge”. In: *Axioms* 11.3 (2022), p. 116. DOI: 10.3390/axioms11030116.

[28] Tao Zheng et al. “Stability and Hopf Bifurcation of a Stage-Structured Cannibalism Model with Two Delays”. In: *International Journal of Bifurcation and Chaos* 31.12 (2021), p. 2150242. DOI: 10.1142/S0218127421502424.

[29] R. Dinnullah. “A Discrete Numerical Scheme of Modified Leslie-Gower with Harvesting Model”. In: *CAUCHY: Jurnal Matematika Murni dan Aplikasi* 5.2 (2018), pp. 65–72. DOI: 10.18860/ca.v5i2.4716.

[30] Prisalo Luis et al. “Implementation of Non-Standard Finite Difference on a Predator–Prey Model Considering Cannibalism on Predator and Harvesting on Prey”. In: *Jambura Journal of Biomathematics (JJBM)* 6.1 (2025), pp. 35–43. DOI: 10.37905/jjbm.v6i1.30550.

[31] Muhammad Ikbal. “Stability Analysis of the Two Prey–One Predator Model with Harvesting of the Prey”. In: *MATHunesa: Jurnal Ilmiah Matematika* 13.3 (2025), pp. 388–394. DOI: 10.26740/mathunesa.v13n3.p388-394.

[32] Aaraf Abdulsatar Alani and Raid Kamel Naji. “The Role of Prey Vigilance, Cannibalism, and Hunting Cooperation on Prey-Predator Dynamics”. In: *Communications in Mathematical Biology and Neuroscience* 2025 (2025), Article ID 112. DOI: 10.28919/cmbn/9513.

[33] Ahmed Sami Abdulghafour and Raid Kamel Naji. “Modeling and Analysis of a Prey–Predator System Incorporating Fear, Predator-Dependent Refuge, and Cannibalism”. In: *Communications in Mathematical Biology and Neuroscience* (2022), Article ID 106. DOI: 10.28919/cmbn/7722.

[34] Dian Savitri and Hasan S. Panigoro. “Hopf bifurcation in the prey-predator-super predator model with different response functions”. In: *Jambura Journal of Biomathematics* 1.2 (2020), pp. 65–70. DOI: 10.34312/jjbm.v1i2.8399.